TEST FAST KICKER PULSER*

W. Zhang, A.V. Soukas, S.Y. Zhang, W.W. Frey, and J. Bunicci

Brookhaven National Laboratory
Upton, New York 11973

ABSTRACT

In this paper, a test pulser of the Brookhaven AGS Booster extraction fast kicker is described. The pulser is projected for both proton and heavy ion operation. A load of total inductance $2.15\mu H$ is used for the test pulser. The PFN voltage is required to be below $40kV$ for operation in air. Rise time of the pulse for proton extraction operation is about $120ns$ up to 97% of full current ($1000A$), and, for heavy ion extraction, $160ns$ up to 98% of full current ($1615A$). R-C compensation networks are used for pulse front edge sharpening. The flexibility of operation is obtained basically by switching an energy dumping resistor to match or mismatch the PFN impedance. Some comments on stray capacitance and stray inductance effects are included.

SYSTEM DESCRIPTION

The Brookhaven AGS Booster extraction kicker magnet, that will be located in vacuum at the F3 straight section of the AGS Booster ring, is required to deflect the 1.5 Gev (rigidity $B_\rho = 7.51 \ T-m$) proton beam by 5 $mrad$, and the 17.5 $T-m$ rigidity heavy ion beam by 3.8 $mrad$. The kicker magnet consists of 4 lumped magnets in series with equal inductances, which are driven by 4 identical pulsers in parallel to provide the required magnetic field during the beam extraction. The pulser voltage is required to be below $40kV$ for operation in air. To meet the requirement of both proton and heavy ion extraction, an energy dumping resistor is switched to match or mismatch the PFN impedance.

The pulser was proposed as basically a regular E-type pulse forming network with equal capacitance and equal inductance for each section. Several R-C compensation circuits are then proposed to sharpen the pulse front edge. The basic circuit diagram is shown in Figure 1.

A test pulser has been built for several purposes. These are: to aid in the design of PFN, to check the computer simulation, to help minimize the values of stray components, and to improve our experience in fast pulse measurements. The load used for the test pulser is a centrally-fed picture frame lumped magnet with a dimension of 28 inches in length. The window size is 5 inches in width and 3 inches in height. The sum of the magnet inductance and pulser loop stray inductance is measured as $2.15\mu H$. The size of the actual Booster kicker magnet will be smaller than the test magnet, therefore for the same performance a little more loop inductance could be tolerated for the kicker pulser.

The test pulser parameters are summarized in Table 1.

Table 1 - Pulser Parameters

	Proton	Heavy Ion
Rise time	120ns (0-97%)	160ns (0-98%)
PFN voltage	6.8kV (34kV)*	11.3kV (36.5kV)*
Peak current	200A (1000A)*	500A (1615A)*
Pulse Length	>600ns	>600ns
Flat top ripple	1.5%	1%
Pulse overshoot	3%	2%

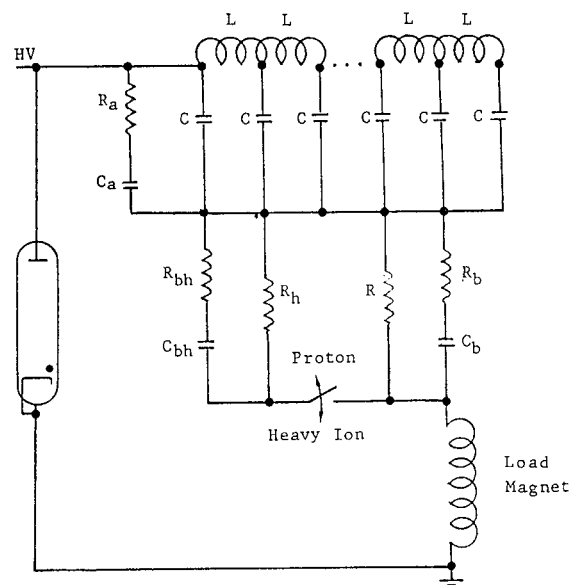*Test parameter (projected parameter).

Figure 1 - Circuit Diagram of Test Pulser

DESIGN AND TEST CONSIDERATIONS

Pulse Shaping

Pulse front edge sharpening, i.e., to extend the linear portion of the sine curve during the pulse rise period, is of primary interest in the design. It has been noticed that on the front edge of the pulse the time spent from 75% to 98% of the full current could be as long as that from 0 to 75% in the uncompensated circuit. Two R-C compensators are, therefore, used to improve the performance.

The R_a-C_a in parallel with the first PFN capacitor is a speed up network. It provides additional energy needed to build up the current of the load magnet during the later portion of the pulse rise period. The proper selection of R_a-C_a will give a faster rising front edge current with the acceptable overshoot or even without an overshoot.

Since the impedance matching resistor has been used, it is proposed to use an R_b-C_b network, that is in parallel with the matching resistor, as a sink network. The capacitance of C_b together with the magnet inductance constitute a resonant network that reduces the resistance to the energy discharging of the PFN front edge capacitor during the pulse rising period. The damping resistor R_b is used to avoid possible oscillation in the L-C network, and its value should be much smaller than that of the impedance matching resistor. During the flat top of the pulse, both C_a and C_b hold at the constant voltages, therefore the pulse flat top is not affected.

In the design, we are using both the sink network and the speed up network.

Report Documentation Page

1. REPORT DATE	2. REPORT TYPE	3. DATES COVERED
JUN 1989	**N/A**	**-**

4. TITLE AND SUBTITLE	5a. CONTRACT NUMBER
Test Fast Kicker Pulser	5b. GRANT NUMBER
	5c. PROGRAM ELEMENT NUMBER

6. AUTHOR(S)	5d. PROJECT NUMBER
	5e. TASK NUMBER
	5f. WORK UNIT NUMBER

7. PERFORMING ORGANIZATION NAME(S) AND ADDRESS(ES)	8. PERFORMING ORGANIZATION REPORT NUMBER
Brookhaven National Laboratory Upton, New York 11973	

9. SPONSORING/MONITORING AGENCY NAME(S) AND ADDRESS(ES)	10. SPONSOR/MONITOR'S ACRONYM(S)
	11. SPONSOR/MONITOR'S REPORT NUMBER(S)

12. DISTRIBUTION/AVAILABILITY STATEMENT
Approved for public release, distribution unlimited

13. SUPPLEMENTARY NOTES
See also ADM002371. 2013 IEEE Pulsed Power Conference, Digest of Technical Papers 1976-2013, and Abstracts of the 2013 IEEE International Conference on Plasma Science. Held in San Francisco, CA on 16-21 June 2013. U.S. Government or Federal Purpose Rights License.

14. ABSTRACT
In this paper, a test pulser of the Brookhaven AGS Booster extraction fast kicker is described. The pulser is projected for both proton and heavy ion operation. A load of total inductance 2.15pJJ is used for the test pulser. The PFN voltage is required to be below 40k V for '?peration i_n ai:. Rise time of the pulse for proton extractiOn operatiOn IS about 120ns up to 97% of full current (lOOOA), and, for heavy ion extraction, lBOns up to 98% of full current (1B15A). R-C compensation networks are used for pulse front edge sharpening. The flexibility of operation is obtained basically by switching an energy dumping resistor to match or mismatch the PFN impedance. Some comments on stray capacitance and stray inductance effects are included.

15. SUBJECT TERMS

16. SECURITY CLASSIFICATION OF:			17. LIMITATION OF ABSTRACT	18. NUMBER OF PAGES	19a. NAME OF RESPONSIBLE PERSON
a. REPORT **unclassified**	b. ABSTRACT **unclassified**	c. THIS PAGE **unclassified**	**SAR**	**4**	

Simulation

To select the right compensation parameters, computer simulation with some mathematical programs has been used for analysis. The fundamental model is in the state space realizations of the pulser. The state space realization of the regular PFN circuit, as shown in Figure 2, is usually presented in a tri-diagonal form. The state space realization of the circuit in Figure 3 can be given in a similar form.
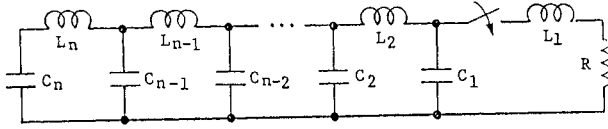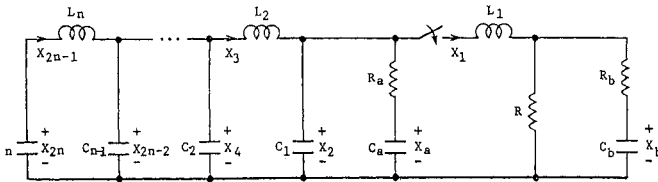

Figure 2

Figure 3

$$\dot{x} = Ax + Bu$$
$$y = Cx + Eu$$

where:

$$x = [\, x_b \; x_a \; x_1 \; x_2 \; \cdots \; x_{2n} \,]^T$$

$$C = [\, 0 \;\; 0 \;\; 1 \;\; \cdots \;\; 0 \,].$$

The matrices B and E are immaterial when only the initial state (zero input) response is concerned. The time response of the output y, i.e., the magnet current, therefore can be derived as

$$y(t) = V \sum_i e^{-d_i t} (\, a_i \cos \omega_i t + b_i \sin \omega_i t \,),$$

where V is the initial state voltage of the PFN capacitor; a_i and b_i are the amplitude associated with cosine and sine terms, respectively; d_i denotes the damping factor, and ω_i is the radial frequency.

The following parameters were used to compare the regular and the compensated current waveforms of a PFN with $(n = 7)$.

$$L_1 = 2600nH \, , \quad R = 18 ohm$$
$$L_2 = \cdots = L_7 = 990nH$$
$$C_1 = \cdots = C_7 = 3.05nF$$
$$R_a = 30 ohm \, , \quad C_a = 0.3nF$$
$$R_b = 1.0 ohm \, , \quad C_b = 1.05nF$$

The coefficients of the time response of the magnet current for the two circuit configurations are listed in Table 2. The left column is for the compensated network, and the right column for the uncompensated case.

Table 2 - Time Response Coefficients

Damping factor:	Damping factor:
d(i) =	d(i) =
1.0e+008 *	1.0e+006 *
0.00011726549356	0.00671418377610
0.00046068624578	0.02917421704174
0.00105463692599	0.07600549240394
0.00213411473497	0.16918641185347
0.02193178073077	1.98071388936207
0.01004740110135	0.83361694724814
0.00449942548135	0.36612731985300
1.21720721859919	
0.42759974609915	

$$A = \begin{bmatrix} \dfrac{-1}{(R+R_b)C_b} & 0 & \dfrac{R}{(R+R_b)C_b} & 0 & 0 & 0 & 0 \\[2mm] 0 & \dfrac{-1}{R_a C_a} & 0 & \dfrac{1}{R_a C_a} & 0 & 0 & 0 \\[2mm] \dfrac{-R}{(R+R_b)L_1} & 0 & \dfrac{-RR_b}{(R+R_b)L_1} & \dfrac{1}{L_1} & 0 & 0 & 0 \\[2mm] 0 & \dfrac{1}{R_a C_1} & \dfrac{-1}{C_1} & \dfrac{-1}{R_a C_1} & \dfrac{1}{C_1} & 0 & 0 \\[2mm] 0 & 0 & 0 & \dfrac{-1}{L_2} & 0 & \dfrac{1}{L_2} & 0 \\[2mm] 0 & 0 & 0 & 0 & \dfrac{-1}{C_2} & 0 & \dfrac{1}{C_2} \\ & & & & & \ddots & \\ & & & & & & \dfrac{-1}{L_n} & 0 & \dfrac{1}{L_n} \\ & & & & & & 0 & \dfrac{-1}{C_n} & 0 \end{bmatrix}$$

726

Radial frequency:

w(i) =

   1.0e+007 $*$

     3.54879899947476
     3.28215199406595
     2.85737172414070
     2.30256805639487
     0.27122591739610
     0.94911987172858
     1.65325870447173

Radial frequency:

w(i) =

   1.0e+007 $*$

     3.55128588723611
     3.29087079307302
     2.87255093133977
     2.31951867405523
     0.26473438663089
     0.94830812250680
     1.66384876749066
     0
     0

Amplitude (Cosine):

a(i) =

     0.00000817740888
     0.00004303049038
     0.00015671961505
     0.00056338193408
    -0.01474893198284
     0.01000759631552
     0.00220615789166
     0.00000213606942
     0.00176173225786

Amplitude (Cosine):

a(i) =

     0.00000931389811
     0.00004613233955
     0.00015093858106
     0.00047287705933
    -0.00999842688004
     0.00765151815920
     0.00166764684279

Amplitude (Sine):

b(i) =

     0.00001723115311
     0.00008540849756
     0.00027424559336
     0.00079658037603
     0.10301001288047
     0.00958890891258
     0.00236222242485
     0.00000000000000
     0.00000000000000

Amplitude (Sine):

b(i) =

     0.00001883356222
     0.00008712541192
     0.00025321488412
     0.00066643933726
     0.09140891615410
     0.00763132616840
     0.00187913735175

Note that the amplitude of the sine term associated with the dominant frequency has been increased about 10% by the compensation.

With the initial state voltage of the PFN capacitors being $V = 36kV$, the current waveforms of the two circuits are shown in Figure 4. At the critical point (i.e., 98% of the full current), the response of the compensated network leads the regular one by more than $90ns$.

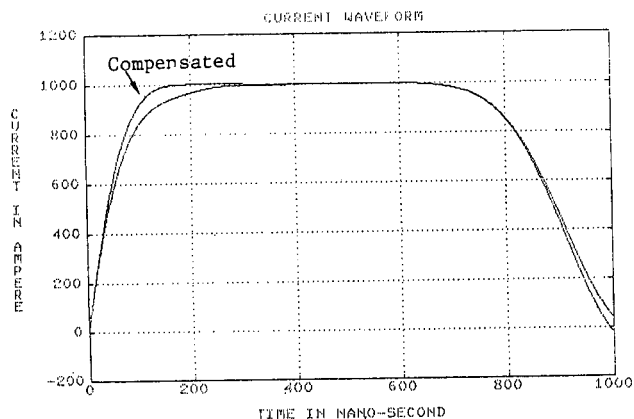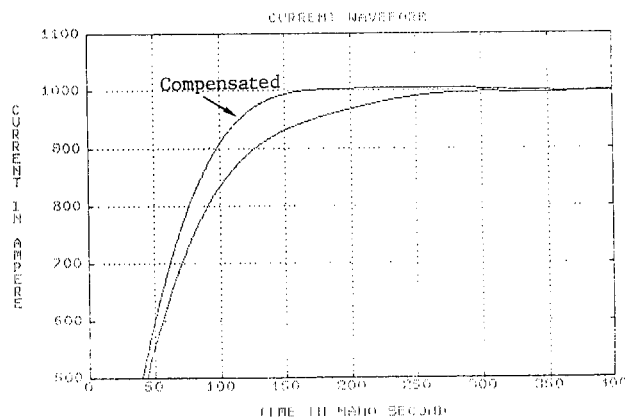Figure 4a

Figure 4b

Stray Inductance and Stray Capacitance Effects

Some investigation of the system distributed parameter effects has been conducted in the earlier tests. Its purpose is to provide understanding and necessary information in the pulser design. Computer simulations have been used for the circuit analysis.

The system stray inductance of the pulser unit, that includes the external loop and thyratron tube inductance, the vacuum chamber feed-through and magnet conductor loop inductance, and the series inductance of the pulse capacitors, has been evaluated based on the existing AGS E5/H5 pulser and the test setups. To reduce the stray inductance of the discharging path, the centrally-fed picture frame magnet structure has been selected. Also the thyratron assembly is constructed as a coaxial structure, and the loop inductance is kept as low as possible.

The pulse distortion due to the mutual inductance of the PFN inductors and the serial inductance of the pulse capacitors has been observed in the test. The pulse overshoot caused by these inductances is usually overlooked in slow rising pulses. For a fast rising pulse, the effect may be so serious that the waveform is spoiled. To resolve the problem, these distributed factors have been simulated in the program, to the point where waveforms generated by the simulation program are consistent with the real waveforms. Therefore, with this understanding, compensation schemes and parameter adjustments aimed at overcoming this problem has been studied by both testing and computer simulation.

The major sources of the stray capacitance in the pulser are the vacuum chamber feed-through, the capacitance between the PFN common plate and the ground plate, and the capacitor cases to the thyratron cathode plate. Depending on its magnitude, stray capacitance will have a variety of effects on the circuit performance. The test and computer simulation results have clearly indicated that pulse flat top ripples are not only due to the PFN characteristics but also due to stray capacitance. The chamber feed-through capacitance, in our case, is the main cause of the flat top ripple.

TEST RESULTS

In our pulser testing, various R-C compensations have been used with different pulse forming networks. The computer simulation of test pulser is shown in Figure 5, which is from Microcap II. The parameters of the network are as follows:

$$L_1 = 2.15\,\mu H\ ,\quad R = 14\,ohm$$
$$L_2 = 810nH\ ,L_3 = \cdots = L_9 = 510nH$$
$$C_1 = C_2 = \cdots = C_9 = 3.3nF$$
$$L_s = 70nH\ (mutual\ inductance\ between\ inductors)$$
$$L_c = 40nH\ (series\ inductance\ of\ PFN\ capacitors)$$
$$R_a = 22ohm\ ,\quad C_a = 1.8nF$$
$$R_b = 1.0ohm\ ,\quad C_b = 2.0nF$$

The test result of pulse front shaping based on the above parameters is shown in Figure 6a. The picture shown in Figure 6b is with same PFN but different sink network and a mismatched resistor. Another test based on a PFN with capacitor value of $3.8nF$ is shown in Figure 7.
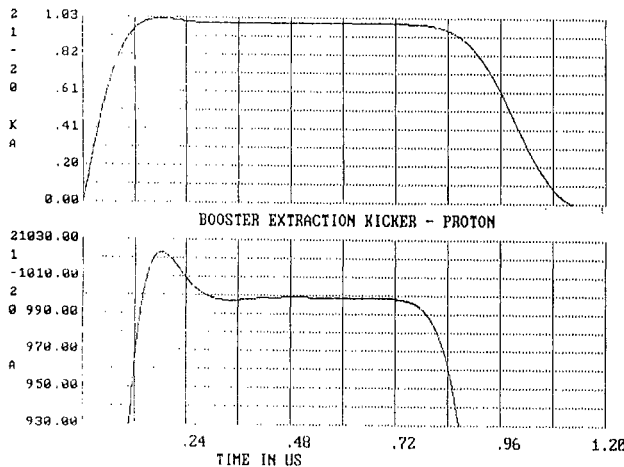
Figure 5 - Simulation

CONCLUSION

The test pulser with lumped magnet is a relatively low cost, small sized system. The test results obtained are basically matched with the computer simulations.

Reference

1. R.M. Nelms, etc., "Simulation of Transmission Line Transients Using a Personal Computer", Proceedings of the 18th Power Modulator Symposium, 1988.

2. R.M. Martinelli, "A State Variable Modeling Technique for Personal Computer Simulation of Converter Dynamic Properties", Proceedings of Powercon 11, 1984.

3. W. Zhang, etc., "Mathematical study and programming methods of pulse forming network - Part I", internal technical note, to be published.
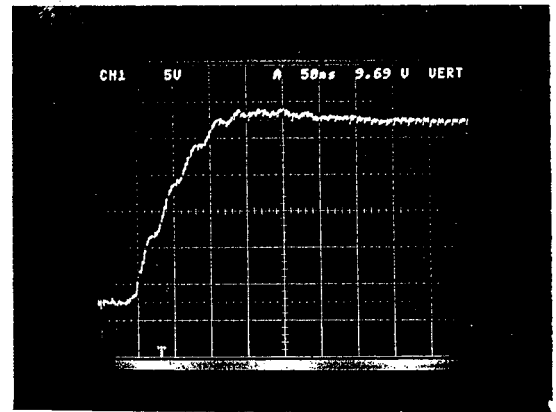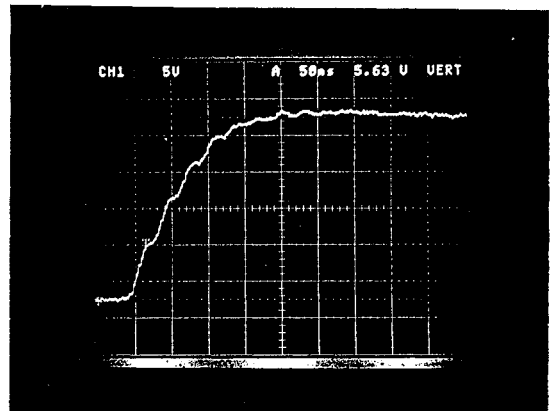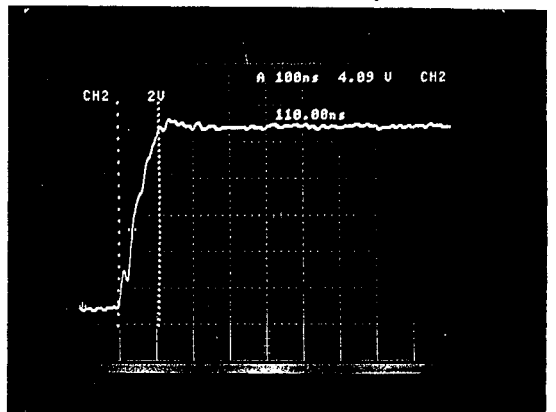
Figure 6a - Proton

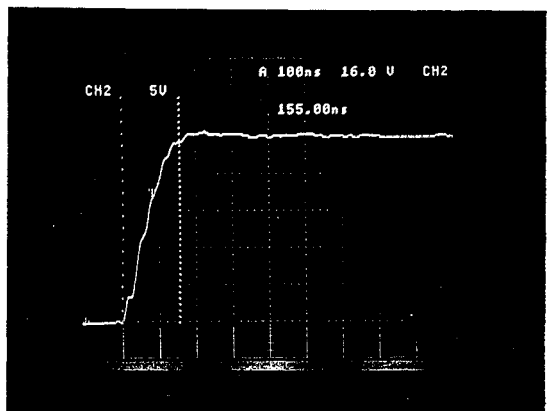Figure 6b - Heavy Ion

Figure 7a - Proton

Figure 7b - Heavy Ion

728